ELSEVIER

Journal of Chromatography A, 796 (1998) 81–99

JOURNAL OF CHROMATOGRAPHY A

Effect of radial gradient of temperature on the performance of large-diameter high-performance liquid chromatography columns I. Analytical conditions

O. Dapremont[a,*], G.B. Cox[a,1], M. Martin[b], P. Hilaireau[a], H. Colin[a]

[a]*Prochrom R&D, 5 Rue Jacques Monod, 54250 Champigneulles, France*

[b]*Ecole Supérieure de Physique et de Chimie Industrielles, Laboratoire de Physique et Mécanique des Milieux Hétérogènes, 10 Rue Vauquelin, 75231 Paris Cedex 05, France*

Abstract

The performance of a large-diameter chromatographic column can be drastically reduced when the solvent enters the column at a temperature different from that of the wall of the column. A radial temperature gradient inside the column will affect the physical properties of the solvent and the chromatographic behaviour of the solute resulting in a deformation of the band profile. A mathematical model is proposed to take into account the effect of a radial gradient of temperature in a large-diameter column on the chromatographic peak shape under linear conditions. The model is then compared with experimental results in preparative columns of different sizes. A good agreement between experiment and theory has been found showing a serious effect of thermal conditions on separation quality, depending on the column size. It is also demonstrated that a small difference of temperature can be helpful to compensate practical effect of frits and distribution of the sample at the extremities of the packed bed. Finally, it demonstrates the necessity to perform efficiency measurement under different thermal conditions to have a good comparison between columns. © 1998 Elsevier Science B.V.

Keywords: Preparative chromatography; Mathematical modelling; Temperature gradients

1. Introduction

The sources of band broadening in a chromatographic column have been thoroughly investigated over the years [1–23]. The increase of the band width can be due to the column itself because of bad packing procedure, poor distribution of the sample or heterogeneity of the bed. It can also be due to an external source of band broadening such as dead volumes, the injection volume, or the detector cell volume [1–13]. In the last decade the effect of certain conditions of solvent and column temperature on variation of column efficiency has been studied [14–18]. These changes in efficiency were attributed to the change of temperature inside the column due to viscous heat generation. This source of band broadening was intensively studied and mathematical models were developed to calculate the temperature profile in two dimensions in an adiabatic analytical column [14–18]. This problem can be easily solved by adequate thermostatting of the solvent at a temperature below the column oven temperature. Recent experimental work conducted on a preparative-scale column has demonstrated the effect of

*Corresponding author. Present address: Chiral Technologies Europe, Boulevard Gonthier d'Andernach, B.P. 167, 67404 Illkirch Graffenstaden, France.

[1]Present address: Chiral Technologies Europe, Boulevard Gonthier d'Andernach, B.P. 167, 67404 Illkirch Graffenstaden, France.

0021-9673/98/$19.00
PII S0021-9673(97)01067-4

a temperature difference between the column wall and the solvent inlet ΔT on the column efficiency [19–22]. In preparative size equipment a temperature difference can be generated by solvent mixing (exothermic or endothermic), modification of the solvent storage temperature or of the column room temperature, and heating of the solvent due to heat generated by the pump, for example. Because the thermal conductivity of the porous bed is rather small compared to that of stainless steel [14–18], and because the flow velocity inside the column is small with little radial mixing (plug flow), the transfer of heat in the chromatographic bed is slow and radial temperature gradients can be observed [20,22]. These radial gradients are responsible for broadening of the sample band inside the column by changing the local velocity and the retention parameters [19–22].

The purpose of this paper is to extend the mathematical model that allows the calculation of the temperature profile in a chromatographic column to the determination of the analytical chromatogram of a single solute in a preparative size column. The calculation results are then compared to experimental data.

2. Theory

In order to calculate the chromatographic peak shape resulting from a column with a radial gradient of temperature it is necessary to solve the mass balance and thermal balance equations for the column. The mass balance equation under non-isothermal conditions in a chromatographic column has not yet been solved. A numerical solution necessitates the resolution of a set of differential equations under non-steady-state conditions. This calculation is not trivial and requires a large computer capacity. The situation can be simplified if the concentration of the sample within the column and its heat of adsorption are small, when one can solve the two balance equations separately. The thermal balance equation has been intensively studied and an analytical solution can be found in the literature [14–18]. We propose here a model to calculate the chromatographic peak of a single solute under linear conditions when the column is not used under isothermal conditions.

2.1. General description of the model

A chromatographic peak under linear conditions can be modelled by a Gaussian distribution. The peak is then defined by a set of two values: the retention time corresponding to the apex of the peak and the variance of the distribution corresponding to the broadening of the peak. In order to calculate peak shape in non-homogeneous columns, Yun and Guiochon [23] considered the chromatographic column equivalent to a set of concentric homogeneous annuli. Each annulus is considered equivalent to a column. This model assumes that there is no radial diffusion of the sample along the column. They could then calculate the chromatogram in each elementary column and hence the total chromatogram (Fig. 1). If one uses such an annulus model, coupled with the analytical solution of the thermal balance equation in the column, one can calculate the chromatographic peak under non-isothermal conditions.

In a large-diameter column when the solvent entering the column is at a different temperature from that of the wall of the column (in this paper this is described by ΔT, which is the difference between the temperature of the column at the wall and the temperature of the solvent at the inlet of the column, which is then positive when the wall is warmer than the solvent), the temperature gradient that exists inside the porous bed is steepest close to the column wall [14–22]. The annulus model was modified to take this observation into account. Instead of a constant radial step to define the relative position of each annulus, we have maintained constant area annuli. The closer to the column wall the thinner is the annulus. This allows a better modelling of the area in which the temperature gradients are steepest. The temperature in each annulus can be considered constant and equal to the averaged temperature across the bed length in the annulus. The two parameters of the Gaussian distribution can then be calculated at the defined temperature. The calculation of the main chromatogram is then straightforward.

2.2. Temperature profile in a large-diameter column

2.2.1. Analytical solution

To calculate the temperature profile inside a

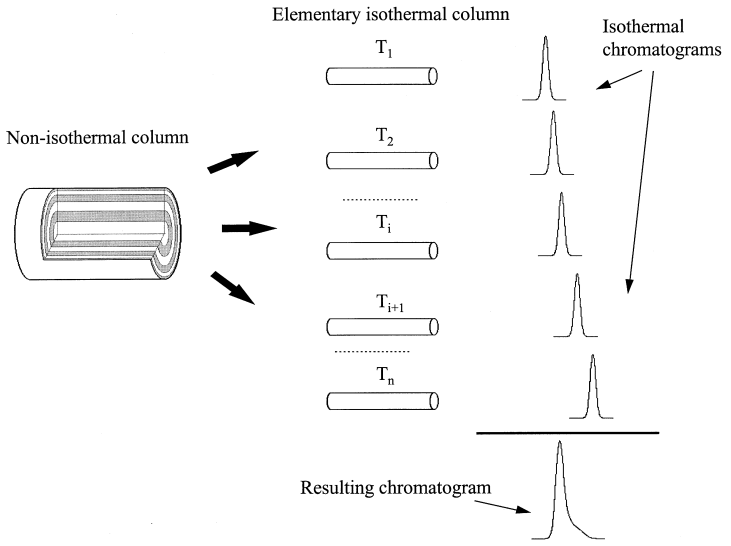

Fig. 1. Principle of the annuli method for the calculation of a chromatogram in a radially non-homogeneous column.

chromatographic column, we have used the analytical solution developed by Poppe et al. [17] extended to the case when the column wall is at a temperature different from that of the solvent entering the column [18]. This model is based on the following thermal balance equation in a porous chromatographic bed in cylindrical co-ordinates:

$$\overline{\rho C_p}\frac{\partial T}{\partial t} = \overline{\lambda_{lon}}\frac{\partial^2 T}{\partial^2 t} + \overline{\lambda_{rad}}\left(\frac{\partial^2 T}{\partial r^2} + \frac{1}{r}\frac{\partial T}{\partial r}\right) - v_s \rho_m C_{pm}\cdot\frac{\partial T}{\partial z} + v_s \cdot\frac{\partial p}{\partial z} \quad (1)$$

in which $\overline{\rho C_p}$ is the average heat capacity per volume for the heterogeneous system, T is the temperature, r is the radial distance from the column axis, z is the axial distance from the column inlet, $\overline{\lambda_{lon}}$ and $\overline{\lambda_{rad}}$ are, respectively, the longitudinal and the radial average effective heat conductivities of the column content, ρ_m is the density of the mobile phase, C_{pm} is the heat capacity of the mobile phase, v_s is the superficial flow velocity and p is the pressure.

The left-hand term corresponds to the accumulation of heat in the column, the first and second terms on the right hand side of the equation correspond to, respectively, the axial and the radial conductions of heat, the third term corresponds to the heat convected by the flow of solvent through the chromatographic bed, and the last term represents the heat generated by viscous dissipation. Assuming a steady state, the non-compressibility of the solvent and a negligible resistance of heat transfer at the column wall, one can solve Eq. (1). The temperature T at any set of co-ordinate (r,z) can be calculated, using the following equation [18], as a function of the temperature of the solvent at the column inlet T_s, the temperature of the column wall T_w and the column radius R_c:

$$T(r,z) = T_w + \Delta\cdot\left\{1 - \left(\frac{r}{R_c}\right)^2 + \sum_{i=1}^{i=\infty}\left(\frac{-8}{\alpha_i^3} + \frac{2(T_s - T_w)}{\alpha_i \Delta}\right)\cdot\frac{J_0\left(\alpha_i\cdot\frac{r}{R_c}\right)}{J_1(\alpha_i)}\cdot\exp(-\alpha_i^2\xi)\right\} \quad (2)$$

with

$$\Delta = v_s.\frac{\Delta P}{L_{col}}\cdot\frac{R_c^2}{4\overline{\lambda_{rad}}} \quad (3)$$

$$\xi = z\cdot\frac{\overline{\lambda_{rad}}}{v_s \rho_m C_{pm} R^2} \quad (4)$$

$J_0(x)$ and $J_1(x)$ are Bessel functions of the first kind and, respectively, of zero and first orders.

Table 1
Values of α_i, roots of $J_0(x)=0$

i	α_i
1	2.4048
2	5.5201
3	8.6537
4	11.7915
5	14.9309
6	18.0711
7	21.2116
8	24.3525
9	27.4935
10	30.6346
11	33.7758
12	36.9171
13	40.0584
14	43.1998
15	46.3412
16	49.4826
17	52.6241
18	55.7655
19	58.9069
20	62.0485
. . .	. . .
$i+1$	$\alpha_i+3.14159\ldots$

The different values between two consecutive values of i tend to the value π (3.14159 . . .) when i becomes large.

The α_i values are positive solutions of the equation $J_0(x)=0$ (see Table 1).

The average radial thermal conductivity in a porous media is difficult to know with accuracy. It is commonly stated, by analogy with mass transfer, that the effective thermal conductivity is the combination of a static term (conduction) and a dynamic term (convection) [14,17]. In liquid chromatography the velocity of the mobile phase is usually very low (few centimetres per minute), hence the static thermal conductivity of the porous media can be a good approximation of the effective radial and axial thermal conductivity. The bed is a mixture of a porous solid and a liquid, as a consequence the determination of the thermal conductivity of such a mixture is not easy. Poppe et al. [17] take, as a first approximation, the solvent thermal conductivity, justifying that by the low thermal conductivity of the silica and the large value of the porosity. An alternative to that solution is to use a model such as the Maxwell model (Eq. (5)), allowing the calculation of an average thermal conductivity of the porous media knowing the thermal conductivity of the fluid phase (λ_f), the thermal conductivity of the solid phase (λ_s) and the porosity of the bed (ϵ_{tot}) [15]:

$$\overline{\lambda_{rad}} = \lambda_f \cdot \frac{(3\lambda_s - 2\epsilon_{tot}(\lambda_s - \lambda_f)}{(3\lambda_f + \epsilon_{tot}(\lambda_s - \lambda_f)} \quad (5)$$

This equation shows that the assumption made by Poppe et al. is reasonable since the thermal conductivity of the silica is very small.

2.2.2. Relaxation length

Poppe et al. [17] defined a specific value of the position z in the column, for which the term in the exponential function in Eq. (2) is reduced by a factor e for the first term of the infinite summation. This value is called the relaxation length l_{relax}, and can be calculated using Eq. (6):

$$l_{relax} = \frac{v_s}{6} \cdot \frac{\rho_m C_{pm}}{\overline{\lambda_{rad}}} \cdot R_c^2 \quad (6)$$

The ratio $\rho_m C_{pm}/\overline{\lambda_{rad}}$ can be considered equivalent to the inverse of a thermal diffusivity. The multiplication of that term by the square of the radius gives a time. This value corresponds to the time necessary for the wall temperature to influence a distance equivalent to the radius of the column. The relaxation length can then be defined as the length required for the chromatographic bed to be influenced by the column wall temperature over a distance, from the wall, corresponding to the value $R_c/\sqrt{6}$.

Fig. 2 shows the value of l_{relax} calculated for different column radii and for various solvents with the linear velocity kept constant. The value for an analytical-size column (4.6 mm I.D.) is only a few centimetres, which is much less than the average column length. For a larger I.D. the relaxation length is much greater. This means that in a small-diameter column the wall temperature rapidly influences the chromatographic bed; this is not the case in a large-diameter column where only a fraction of the solvent is influenced by the wall temperature.

2.2.3. Average axial temperature

In a large-diameter column the radial temperature profile will not change drastically over the entire length of the bed [19–21], so one can calculate a mean temperature averaged over the column length at a given radial position. This integration leads to

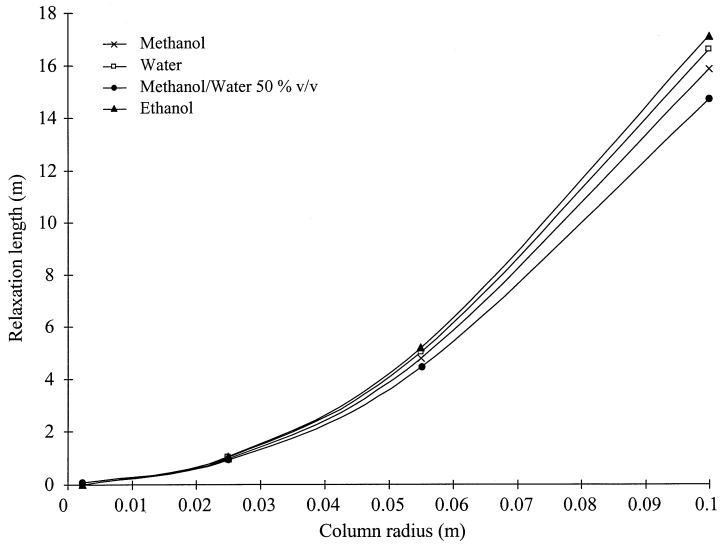

Fig. 2. Relaxation length (Eq. (6)) for different solvents and various column diameter at constant velocity (0.0585 cm/s).

the following equation where ξ_L correspond to ξ for $z=L_{col}$:

$$\bar{T}(r) = T_w + \Delta \cdot \left\{ 1 - \left(\frac{r}{R_c}\right)^2 + \sum_{i=1}^{i=\infty} \left(\frac{-8}{\alpha_i^3} + \frac{2(T_s - T_w)}{\alpha_i \Delta} \right) \cdot \frac{J_0\left(\alpha_i \cdot \frac{r}{R_c}\right)}{J_1(\alpha_i)} \frac{[1 - \exp(-\alpha_i^2 \xi_L)]}{\alpha_i^2 \xi_L} \right\} \quad (7)$$

Eq. (7) exhibits the same characteristics as Eq. (2) and will be used to calculate the average temperature in the elementary column corresponding to the annulus located at the desired radial position.

It is more accurate to determine the axial average temperature at a radial position that gives the correct retention time. This calculation is not explicit and requires an iterative procedure. The increase in the calculation time required is not compensated by any significant gain in the accuracy of the result.

2.2.4. The wall temperature effect

To evaluate the width of the zone influenced by the wall temperature, one can calculate a radial position for which the temperature in the chromatographic bed corresponds to a certain value $T_{(r,z)}$ at a given axial position. In other words, instead of a relaxation length corresponding to an exponential decay of the temperature difference at a given radial position ($R_c/\sqrt{6}$), one can determine a radial position for a given length of the column where the temperature has a defined value. One can define δ as the ratio of the difference of the temperature at a given set of positions (r,z) with that at the centre of the column ($T_{(0,z)}$) to the difference between the temperature at the wall (T_w) and the column centre:

$$\delta = \frac{(T_{(r,z)} - T_{(0,z)})}{(T_w - T_{(0,z)})} \quad (8)$$

Eq. (6) establishes a linear relation between the axial position (l_{relax}) and the square of the radial position ($R_c^2/6$), so one can expect a similar relation between the width ($R_c - r_\delta$) of the zone where the temperature gradient is located and the column length.

Fig. 3 represents the evolution of the distance from the wall of the column as a function of the square root of the axial position (z) for a value of δ equal to 0.1 in an 11-cm I.D. column eluted with a mixture of methanol–water (50:50, v/v) at 200 ml/min. The data were determined from temperature profiles calculated at different axial position in the column using Eq. (2), Eq. (3) and Eq. (4). The column length is taken to be equal to 25 cm which is

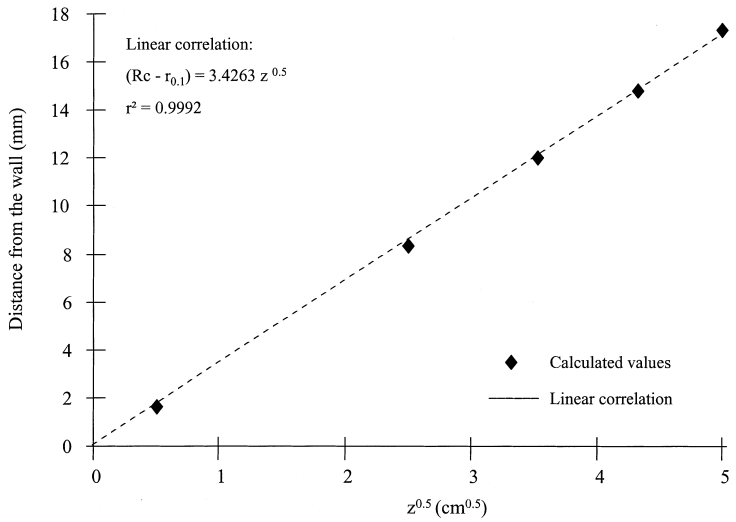

Fig. 3. Wall temperature effect as a function of the column length. Width of the zone from the wall where 90% of the temperature gradient is located as a function of the column length ($\delta = 0.1$ in Eq. (8)). $T_w = 34°C$; $T_s = 20°C$; flow-rate = 200 ml/min; solvent, methanol–water (50:50, v/v).

smaller than the relaxation length (around 5 m) for that particular diameter column, and the linear correlation is calculated assuming that the distance from the wall tends to zero when the axial position tends to zero. This figure shows that the penetration distance of the wall temperature effect increases linearly with the square root of the column length. It also indicates that the first term of the infinite summation is dominant and that the other terms can be neglected to calculate the relaxation length.

2.2.5. Influence of the column diameter

Using Eq. (7) we have calculated the average radial temperature profile in a column 25 cm long at a given linear velocity of the solvent (0.035 cm/s) for different internal diameter values and 14°C difference between the column wall (warmer) and the solvent temperature (Fig. 4). This figure represents the different profiles as a function of the fractional column radius expressed as a percentage. For an analytical column the profile is almost flat over the entire cross-section of the column. One can note that the main part of the temperature gradient represents a smaller percentage of the radius when the column diameter increases. Fig. 5 represents the same results as Fig. 4 but the radial position is expressed as a distance from the wall. Because the linear velocity of the solvent is constant, the rate of heat transfer is the same for all diameters. Fig. 5 shows that the profiles are almost superimposable for large-diameter columns, but the analytical-size column profile is quite different. According to Eq. (6) the relaxation length is much smaller than 25 cm for the 4.6-mm I.D. column and greater than the column length for the other diameters. For the former, the influence of the wall temperature extends to a distance perpendicular to the column wall greater than one radius, which is not the case for the wider columns. Fig. 6 represents schematically the zone which is influenced by the column wall. It shows the boundary between the zone little affected by the wall (to the left of the figure, where the temperature is within 10% of the incoming solvent temperature) and that significantly affected. It also shows the approximate radial temperature profile at certain positions along the column. The figure assumes that the temperature of the solvent inlet (at the left of the figure) is lower than that of the column wall and also that the heat generated by viscous dissipation is important. For an analytical column of diameter 4.6 mm the outlet of the column is located at the right extremity of the figure. In this case the effect of the temperature is

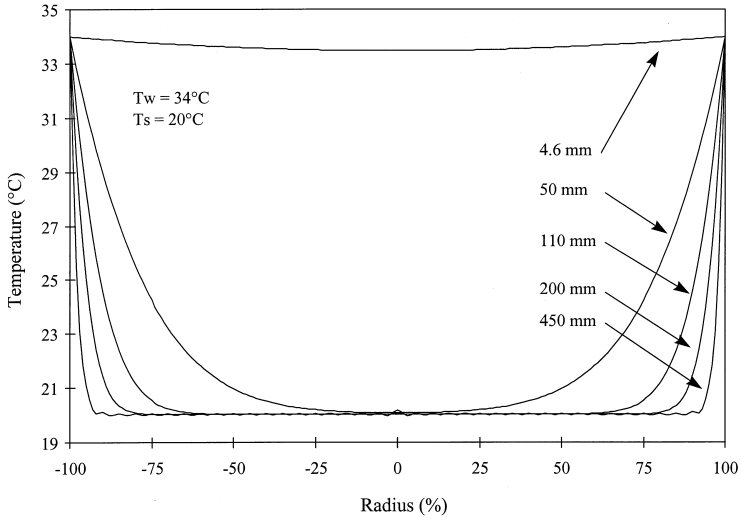

Fig. 4. Average temperature inside a column for different internal diameters as a function of the percentage of the radius. Constant linear velocity, 0.035 cm/s; $T_w = 34°C$; $T_s = 20°C$; column length = 10 cm; solvent, methanol–water (50:50, v/v).

not noticeable because it is compensated over the column length. For a larger-diameter column, with the same linear velocity as the narrower one, the position which corresponds to a length of 25 cm moves to the left of the figure with increasing diameter. It can be seen that the radial temperature profile is increasingly dependent on the inlet boundary conditions for such columns. At the limit when the diameter is very large compared to the column length the elution is mainly controlled by the solvent temperature (left of the figure).

2.2.6. Influence of the flow-rate

As defined by Poppe et al. [17] the relaxation

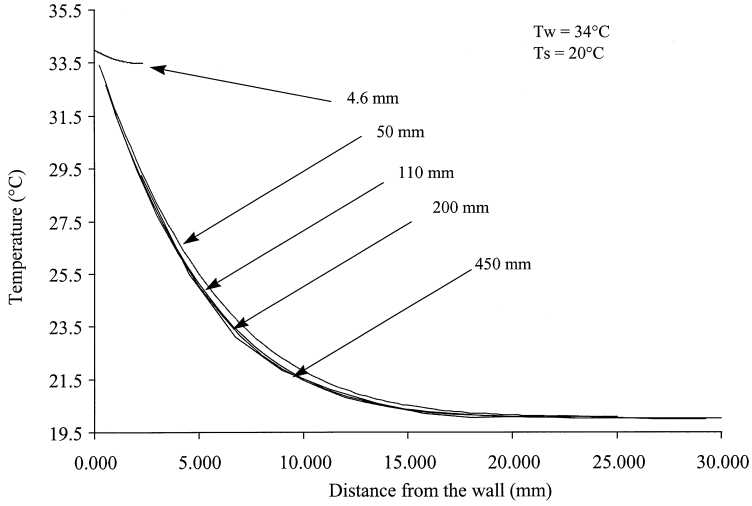

Fig. 5. Average temperature inside a column for different internal diameters as a function of the distance from the wall. Same conditions as Fig. 4.

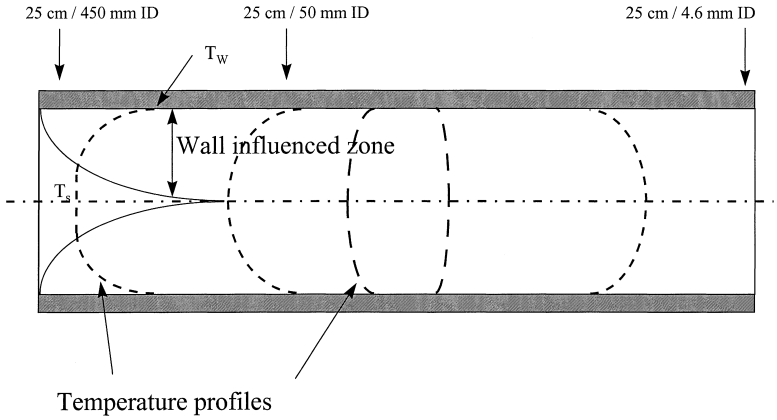

Fig. 6. Representation of the effect of the temperature of the column wall on the internal temperature profile in the column. The dotted lines represent the radial temperature profile. The solid lines represent the limit of the zone influenced by the wall temperature.

length can be expressed as a function of the flow-rate by replacing the velocity and the column radius by the volumetric flow-rate Q_v:

$$l_{relax} = \frac{Q_v}{6\pi} \cdot \frac{\rho_m C_{pm}}{\overline{\lambda_{rad}}} \quad (9)$$

The relaxation length increases with the flow-rate. This means that the length required to observe a certain wall temperature effect ($\delta = 0.1$, for example) at a given radial position increases with the flow-rate. One can define a time t_{th}, corresponding to the time required for heat to diffuse from the wall over a distance for which d takes a value of 0.1 for a given radial position $r_{0.1}$:

$$t_{th} = (R_c - r_{0.1})^2 / \left(\frac{\overline{\lambda_{rad}}}{\rho_m C_{pm}} \right) \quad (10)$$

The time required by the solvent to reach a position z in the column is a function of the linear velocity in the column. The equality of the elution time and the time required for heat to diffuse from the wall leads to Eq. (11), expressing the width of the wall temperature effect as a function of the axial position z and the flow-rate for a value of δ equal to 0.1:

$$(R_c - r_{0.1})^2 = \frac{\overline{\lambda_{rad}}}{\rho_m C_{pm}} \cdot z \cdot \frac{\pi R_c^2}{Q_v} \quad (11)$$

This equation shows that, when the flow-rate tends to an infinite value, the effect of the wall temperature is negligible, but when the flow-rate is small the penetration distance is large.

2.3. Non-isothermal chromatogram

2.3.1. Elementary column

The column is divided into a number of concentric annuli. Each annulus is defined by two radial positions corresponding to the internal and the external cylinder delimiting the annulus. An average radius can be calculated for each annulus by a geometric average of the two values. For that average radial position one can calculate an average temperature along the annulus using Eq. (7). This temperature allows the calculation of the physical properties of the solvent such as viscosity η and density ρ, and the properties of the solute like the retention factor k' and the diffusion coefficient D_m. To obtain an analytical solution of the thermal balance equation, Poppe et al. [17] had to assume the physical properties were independent of the temperature in the domain of calculation. However, one can find in the literature or measure experimentally the variation of the physical properties with temperature. Simple mathematical correlations can be used to fit the data in a narrow range of temperature (10–20°C). It is then possible to calculate a radial profile of viscosity, density, diffusion coefficient and retention factor with the calculated radial temperature profile. This is then in contradiction with the assumption of the temperature model. For the viscosity, for example, a

polynomial of the first order can be used to fit data in the range 20–40°C. The viscosity profile will be of the same shape as the temperature profile, but reversed as seen in a mirror placed perpendicular to the column axis (the viscosity decreases when the temperature increases). The combination of the different profiles will result in a radial velocity profile influencing the shape of the chromatographic peak.

The division of the column into concentric annuli is such that the cross-sectional area of each annulus is constant. This means that the main mass flow can be divided and distributed equally into each annulus, assuming that the pressure is homogeneous over the entire section of the column. The mass flow at the inlet of the column is divided by the number of annuli and transformed into a volumetric flow with the local value of the solvent density for each elementary column.

2.3.2. Elementary chromatogram

An analytical chromatogram can be characterised by a Gaussian distribution assuming that the injected quantity is small enough. The general equation for a Gaussian distribution centred on the value t_R can be expressed as follows:

$$f(t) = \frac{1}{\sigma_{\text{tot},t}\sqrt{2\pi}} \exp\left(- \frac{(t - t_R)^2}{2\sigma^2_{\text{tot},t}} \right) \quad (12)$$

where $\sigma^2_{\text{tot},t}$ is the variance of the distribution expressed in the same units as t_R.

It is necessary to determine the value of both t_R and $\sigma^2_{\text{tot},t}$ for each elementary column. To calculate the retention time it is necessary to evaluate the retention time of an unretained compound $t_{0,j}$. This time can be evaluated for each elementary column using the elementary cross-section S_j (constant), the column length L_{col}, the total porosity ϵ_{tot} and the superficial velocity of the mobile phase:

$$t_{0,j} = \frac{L_{\text{col}} \epsilon_{\text{tot}} S_j}{v_s} \quad (13)$$

The mobile phase velocity in each elementary column is deduced from the viscosity and the volumetric flow-rate with the Darcy equation assuming that the pressure is radially homogeneous.

$$\Delta P = \frac{v_s L_{\text{col}} \eta K_p}{d_p^2} \quad (14)$$

with K_p the parameter of the bed permeability (600 for spherical particles and 1000 for irregular); and d_p the particle diameter.

The retention time $t_{R,j}$ can then be calculated by the following equation knowing the variation of the retention factor with the temperature:

$$t_{R,j} = t_{0,j}[1 + k'_j(T)] \quad (15)$$

The variance of the distribution $\sigma^2_{\text{tot},t,j}$ for the column j can be evaluated by the estimation of the column efficiency using a model such as the well-known Knox model. This model relates the reduced plate height h, to the reduced solvent velocity v:

$$h = Av^{1/3} + \frac{B}{v} + Cv \quad (16)$$

The values of the parameters A, B, and C can be experimentally determined by repeating analytical injections at different flow-rate and temperature. These parameters were measured at 25°C and are considered constant in the range 20–40°C despite the variation of the temperature in the column that may affect the column efficiency [24]. The A term, which describes the state of the packed bed, should be fairly invariant with temperature, and the B term is not significant at normal values of flow-rate. This leaves the C term (for the inter-phase mass transfer), which can be to some extent temperature dependent. The value of this parameter for small molecules in reversed-phase chromatography is small, and therefore the small expected change on the C term with temperature may safely be ignored. The column plate number N_{col} is then calculated by the following equation:

$$N_{\text{col}} = L_{\text{col}}/(hd_p) = t^2_{R,j}/\sigma^2_{\text{tot},t,j} \quad (17)$$

The combination of Eq. (17) and Eq. (16) allows the determination of the variance of the Gaussian distribution:

$$\sigma^2_{\text{tot},t,j} = t^2_{R,j} \frac{d_p}{L_{\text{col}}} (Av^{1/3} + B/v + Cv) \quad (18)$$

Once the retention time and the variance of the

distribution are calculated the chromatogram of a sample in an elementary column is defined.

2.3.3. Total chromatogram

The calculation of the total chromatogram is straightforward. The concentration profile as a function of the time and the injected concentration for each elementary column (i.e. the chromatogram) is defined by the following equation:

$$C_j(t) = \frac{C_{\text{inj}}}{\sigma_{\text{tot},t,j}\sqrt{2\pi}} \exp\left(-\frac{(t - t_{R,j})^2}{2\sigma^2_{\text{tot},t,j}} \right) \quad (19)$$

The main chromatogram is then calculated by the summation of all the $C_j(t)$ functions modified by the volumetric flow-rate in each elementary column.

3. Experimental

3.1. Set-up

Two dynamic axial compression columns (Prochrom, Champigneulles, France) were used (Fig. 7): one of 11 cm internal diameter and with a 15-cm piston stroke length; the other with a conventional LC-50 column with an internal diameter of 5 cm and a stroke length of 50 cm. The maximum bed lengths for the two columns were 10 and 25 cm, respectively; the actual bed length was determined by the quantity of packing used in the preparation of the columns. Each column was equipped with a jacket connected to a thermostatted water bath (Julabo MV-F25 (heating, 2.2 kW; cooling, 0.17 kW); Atelier Cloup, Champigny s/s Marne, France). The flow-rate was selected to ensure a turbulent flow in the jacket. The solvent was pumped through the 5-cm I.D. column with a two-head pump (EKM2 Piston 8 mm, 220 ml/min maximum flow-rate; Lewa, Sartrouville, France) and with a three-head pump for the larger I.D. column (EK3 F808TV/C4 1500 ml/min maximum flow-rate; Lewa). A heat exchanger was placed after the pump and consisted of a coil (1/4 inch I.D.) placed in a thermo-regulated bath (Heto DT, 1.2 kW for 5 cm I.D. column (Atelier Cloup); and a TH30SI (heating, 2 kW; cooling, 1.5 kW) for the 11-cm I.D. column (Maton, Lesquin, France)). The sample was manually injected with a 5-ml syringe through a three-way Whitey valve placed after the heat exchanger. The chromatographic signal was detected with a UV detector (Dynamax UV-1 for the 5-cm I.D. column (Rainin, Woburn MA, USA) and Spectra 100 for the 11-cm I.D. column (Thermo-Separation Physics, Les Ulis, France)). The chromatograms were recorded with Prochrom data acquisition software for the 11-cm I.D. column and with Peak 96 software (Hewlett-Packard, Evry, France) for the 5-cm I.D. column. All solvent lines were insulated. The temperature was measured with PT100 probes connected to a digital display unit (IT2020 Serv'instrumentation, Urigny, France). The probe on the solvent line was located on a T-connector immediately before the sample injection valve to avoid influencing the sample profile. The temperature of the column wall was taken at the outlet of the column jacket. The temperature at the inlet of the jacket was periodically measured. Because stainless steel is a good heat conductor, the temperature of the column wall can be considered equal to the temperature of the jacket outlet stream, assuming that the flow-rate in the jacket is large enough to ensure a good heat transfer and that the difference between the inlet and the outlet temperatures of the jacket is small. Ex-

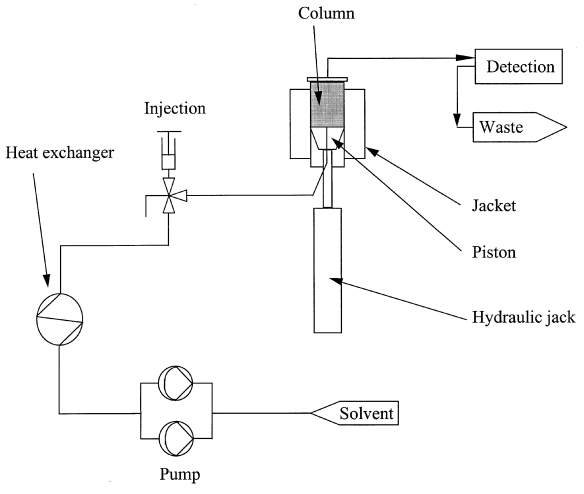

Fig. 7. Experimental set-up.

perimentally that difference was always less than 2°C.

3.2. Chemicals

The eluent used was methanol–water (50:50, v/v). The methanol used was technical-grade purity (SDS, Peypin, France), the water was HPLC grade, produced using ion exchange, activated carbon and reverse osmosis cartridges (Millipore, Molsheim, France). The packing material was a reversed-phase C_{18}, 15-μm average particle size, 100-Å pore size (Amicon, Beverly, MA, USA). The sample used for efficiency determination was a mixture of uracil (Fluka Chemical 94220 No. 282505-689; Sigma–Aldrich, L'Isle d'Abeau, St Quentin Fallavier, France) and acetophenone (Sigma A-1890 No. 84H3402; Sigma–Aldrich) diluted in the elution solvent. The isopropanol used in the packing procedure was technical grade (SDS).

3.3. Procedures

Each column was prepared with a mixture of packing material and 2-isopropanol with the ratio of 1 volume of packing material to two volumes of solvent. The bed was compressed to 25 bar for the 11-cm I.D. column, and 40 bar for the 5-cm I.D. column.

The column dead volume was estimated with the retention time of the uracil (0.22 or 0.1 mg/ml depending on the column I.D.). The uracil is a non-retained compound ($k' \cong 0$) and the acetophenone is retained with a capacity factor close to 2.7 depending on the temperature conditions. The efficiency of the column, N_{col}, is measured by injection of acetophenone (1.2 or 0.5 mg/ml depending on the column I.D.), and measurement of the width of the peak at half height according to the following equation:

$$N_{col} = 5.54 \cdot \left(\frac{t_R}{W_{1/2}} \right)^2 \quad (20)$$

The asymmetry of the peak was measured at 10% of the peak height. For the 11-cm I.D. column, the temperature of the column wall was first maintained at 34°C and the solvent temperature was changed from 20 to 34°C. The wall temperature was then lowered to 25°C to allow the solvent to reach higher temperatures. For the 5-cm I.D. column, the solvent temperature was controlled at 25°C and the column wall temperature was changed from 20 to 34°C. Three sample injections were made for every value of the temperature when it has stabilised. The system was left to equilibrate for at least 30 min per degree of change before any injection. In the following, the difference in temperature between the column wall and the solvent inlet will be referred as ΔT. A positive value of ΔT indicates a higher temperature for the column wall than the solvent line.

4. Results and discussion

4.1. Effect of the temperature difference on column performance

The existence of a temperature difference between the column wall and the solvent at the inlet of the column may be due to many causes, as discussed earlier. That difference introduces a temperature gradient in the column which may influence the velocity profile and hence the solute elution band in the column. The calculation of the temperature profile inside a chromatographic bed using the equations presented in the theoretical part of that paper shows that the temperature difference imposed at the inlet of the column does not vary drastically along the column when the diameter of the column is large. By controlling the temperature of both the solvent line and the column jacket we have investigated the effect of such a temperature difference on the chromatography of a single compound in columns of different size.

Fig. 8 represents the efficiency and the asymmetry of the acetophenone measured in the 11-cm I.D. column as a function of the difference of temperature. The sample is eluted with methanol–water (50:50, v/v) at 200 ml/min. Eq. (20) is only valid when the peak is symmetrical and can be modelled by a Gaussian distribution, hence the values of efficiency shown on Fig. 8 corresponding to values of asymmetry far from unity are not accurate, but are useful to estimate the loss of

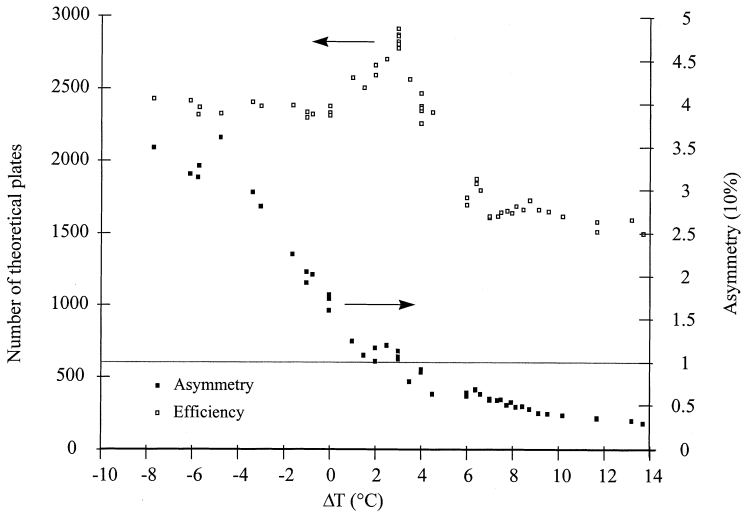

Fig. 8. Effect of ΔT on column efficiency measured at half height of the peak (Eq. (20)) and asymmetry measured at 10% of the peak height. Solute, acetophenone, injection 2 ml at 1.2 mg/ml; column, 10 cm×110 mm I.D.; packing, C_{18}, 15 μm, 100 Å; solvent, methanol–water (50:50, v/v) at 200 ml/min.

performance. This figure shows that the efficiency of the column reaches a maximum for a positive value of ΔT (around 3°C) and is sensitive to a small change in the ΔT value. The efficiency of the column can be divided by a factor of two if the temperature difference is increased only by 3°C; it is clear that measurements of efficiency for wide-diameter columns should be carried out under carefully controlled operating temperatures (as, indeed, should be their operation). One can also note that the efficiency maximum corresponds to a symmetrical peak. The chromatograms corresponding to three specific values of ΔT are shown in Fig. 9. The peak corresponding to a positive value of ΔT exhibits a shoulder in front of the peak. In that case the peak width becomes important affecting the value of the asymmetry. When the ΔT becomes very large the shoulder separates from the peak and a valley appears between the two peaks. When the minimum of the valley drops below the half height of the main peak (the second) the measured efficiency using Eq. (20) increases again. The apparent retention time of the shoulder corresponds to a section of the column influenced by the wall temperature that is warmer than the solvent. When the ΔT is negative the peak is tailing. The model used to calculate the efficiency is then no longer valid which leads to an apparently constant efficiency and hence a plateau on the left part of Fig. 8. These observations lead to the conclusion that the section of the column influenced by the column wall temperature is smaller than the section influenced by the solvent. This can be explained by reference to Fig. 4, which shows the radial temperature profile in a 11-cm column under the same temperature conditions as the experiment. This profile shows that the centre of the column is eluted at the solvent temperature and represents more that 60% of the column radius. The rest of the cross-section is influenced by the temperature gradient. Chromatogram 2 was obtained with a slightly lower flow-rate (184 ml/min) but is presented here to show that a 'normal' peak shape can be obtained with a null ΔT.

Fig. 10 represents the effect of ΔT on the efficiency of the column and the symmetry of the peak calculated for the conditions used for Fig. 8. The parameters of the calculation are summarised in Table 2.

Fig. 10 exhibits the same profile as Fig. 8. The efficiency reaches a sharp maximum corresponding to a symmetrical peak. The main difference between these two figures is the value of ΔT for which the maximum of efficiency can be observed. The calculated data show that the maximum is obtained for a

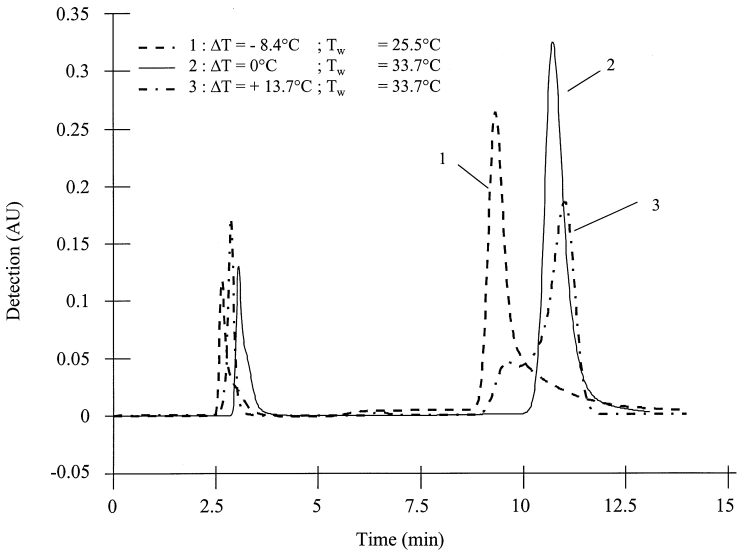

Fig. 9. Chromatograms obtained for three values of ΔT. Same conditions as Fig. 8. First peak uracil, second peak acetophenone. Temperature as indicated on the figure.

null ΔT, but the experimental data give a positive value for the ΔT optimum. This positive value of ΔT required to obtain the maximum of column efficiency has been observed in our early work [19] and also by Brandt et al. [20]. A positive ΔT corresponds to a wall warmer than the solvent, and hence should introduce a radial profile of velocity: the solute close to the wall moving faster than the one in the centre of the column. In order to obtain a symmetrical peak under such thermal conditions it is necessary to have an elution profile at the inlet of the column that is bent in the opposite direction of the radial temperature (i.e. velocity) profile. This can be explained by a distribution effect of the sample across the entire

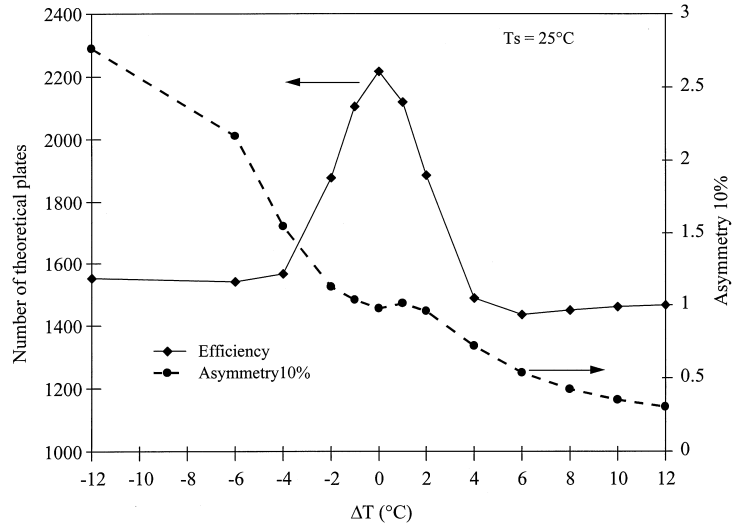

Fig. 10. Calculation of the effect of ΔT on column efficiency measured at half height of the peak (Eq. (20)) and asymmetry measured at 10% of the peak height. Calculation conditions as indicated in Table 2.

Table 2
General set of parameters for the calculation of the chromatogram under non-isothermal conditions

Column	10 cm×110 mm I.D.
Packing	15 μm spherical
Thermal conductivity (W/m/°C)	1.4
Knox parameters	$A=0.88$; $B=2$; $C=0.043$
Solvent	Methanol–water (50:50, v/v)
Viscosity (Poiseuille)	$(13.507-0.039875T)\ 10^{-3}$ (K)
Density (kg/m^3)	$1.1086-0.00066T$ (K)
Specific heat (J/kg/°C)	3768.4
Thermal conductivity (W/m/°C)	0.6
Solute	Acetophenone
Retention (experimental)	$0.0183\exp(-1500/T)$
Diffusion coefficient	Wilke and Chang equation

Correlation and values from Ref. [25].

section of the column. Coq et al. [13] demonstrated the distribution effect due to the change in cross-section when the sample is entering the column. If the flow is considered as a series of parallel streams, a molecule of sample in the central stream reaches the column (after the inlet frit) before the one located in the stream close to the wall. This difference of travel time is due to the difference in the distance which each molecule must cross before entering the column. The one in the centre needs to cross the frit only axially while the one located close to the inlet tube wall must not only cross the frit axially, but needs also to travel radially to reach its inlet position. This phenomenon also occurs at the outlet of the column. As a result, the sample injection band is not perfectly flat as it emerges from the inlet distributor.

The calculated values assume a perfect solute distribution at the inlet of the column and, as a consequence, the maximum efficiency is obtained for isothermal conditions (the distortion of the band due to heat generated by viscous dissipation is very small in the case studied). Experimentally, it is very difficult to get rid of the distortion of the elution profile due to the distribution of the solute and, as a consequence, a positive ΔT is necessary to obtain the maximum efficiency of the column.

Other differences can be observed between Fig. 8 and Fig. 10, but can be related to the approximations made for the calculation, such as constant A, B and C terms in the Knox equation measured at 25°C introducing a difference in the number of theoretical plates calculated. The calculated asymmetry exhibits a plateau around isothermal conditions. This behaviour can be related to the viscous heat generation that becomes less negligible when ΔT is null. The heat generated in that case tends to give a parabolic shape to the radial temperature profile which affects the peak shape and hence the peak symmetry.

4.2. Flow-rate effect

The influence of flow-rate was studied on the 5-cm I.D. column, packed to 22.5 cm length. Three flow-rates were used: 75, 110, 165 ml/min. For each flow-rate value, the efficiency of the column was measured for the acetophenone peak at different values of ΔT. Fig. 11 represents the experimental data obtained, and can be compared to the data calculated for the same conditions with the mathematical model (Fig. 12). The two sets of data (experimental and calculated) are quite similar. Once again the experimental position of the maximum efficiency is obtained when the ΔT is positive, which is not the case for the calculated data. As expected, the maximum values of efficiency are greater at small flow-rates. The position of the maximum efficiency is not significantly influenced by the flow-rate and remains at a ΔT value around 2°C.

4.3. Column length effect

The 5-cm I.D. column was packed to a length of 10 cm and the measurement of column efficiency was conducted at a flow-rate of 75 ml/min using the same conditions as described in Section 4.2. Fig. 13

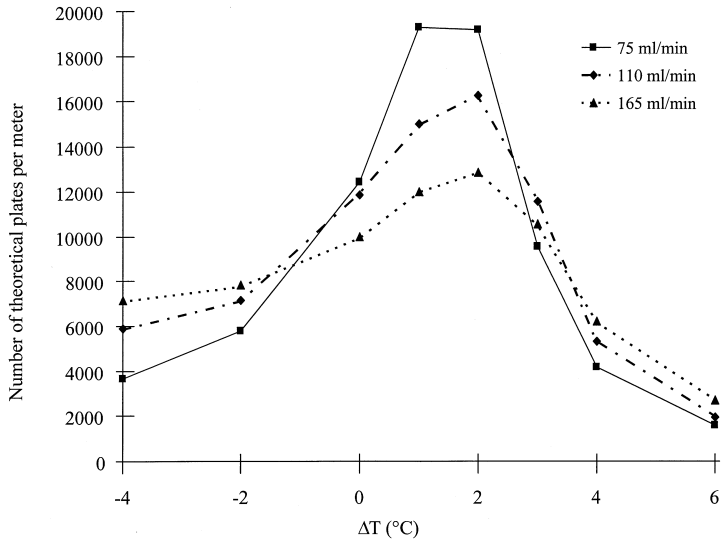

Fig. 11. Effect of the flow-rate on the column efficiency as a function of the ΔT. Solute, acetophenone, 2 ml at 0.5 mg/ml; column, 22.5 cm×50 mm I.D.; packing, C_{18}, 15 μm, 100 Å; solvent, methanol–water (50:50, v/v).

Fig. 14 present, respectively, experimental and calculated data obtained under these conditions. In both figures one can observe that the optimum efficiency is sharper when the column is longer. This is due to the fact that, for the column length employed, the radial temperature gradient is almost constant in such a diameter column. Thus the influence of the wall temperature on the local velocity of the sample is greater for the longer column because the solute travels a greater distance under the radial velocity gradient, resulting in a larger broadening effect of the sample elution band. As already mentioned, a

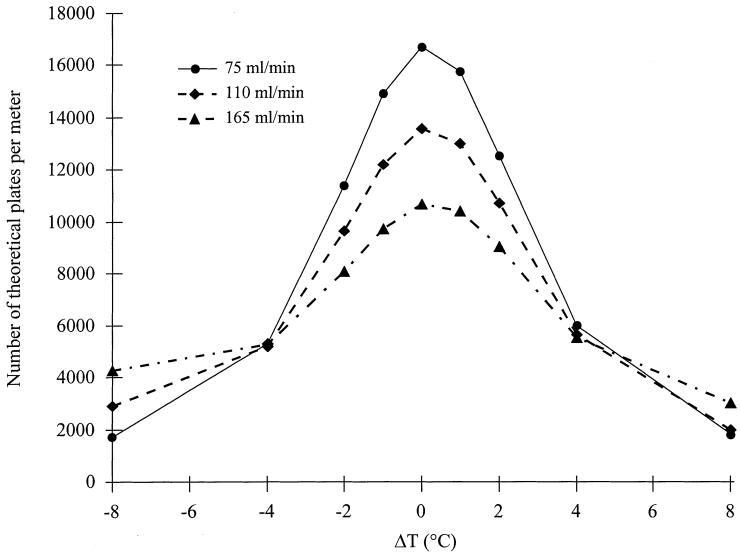

Fig. 12. Calculation of the effect of the flow-rate on the column efficiency as a function of ΔT. Calculation conditions as indicated in Table 2, except for the column dimensions, changed to 22.5 cm×50 mm I.D. to match experimental conditions.

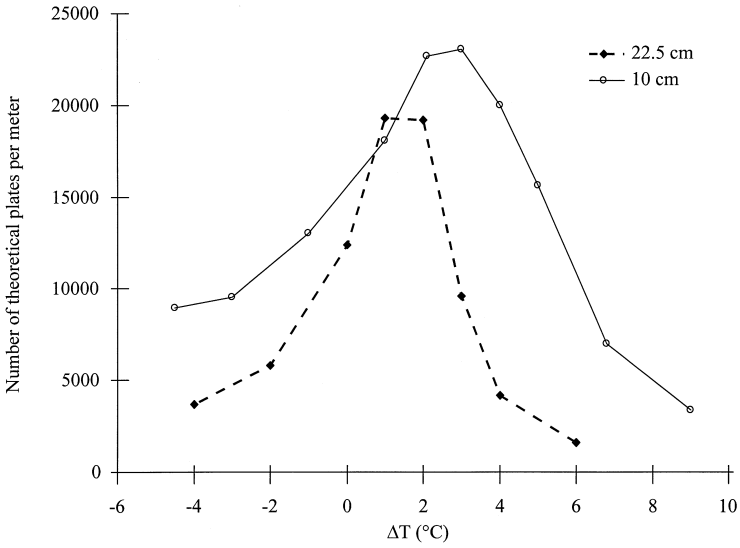

Fig. 13. Effect of the bed length on the column efficiency as a function of ΔT. Solute, acetophenone, 2 ml at 0.5 mg/ml; column, 50 mm I.D.; packing, C_{18}, 15 μm, 100 Å; solvent, methanol–water (50:50, v/v) at 75 ml/min.

positive ΔT is necessary to obtain the maximum efficiency. This is not observed for the calculated data. One can note that the ΔT required for optimal efficiency for a short column is larger than for the long column. As noted above, the need for a difference in temperature is a direct consequence of the deformation of the band due to the extremities of the column. For both lengths, the deformation is the same, but the time available for the sample at the wall to catch up with the sample in the centre of the column depends on the length of the column. When the column is short it is necessary for the sample

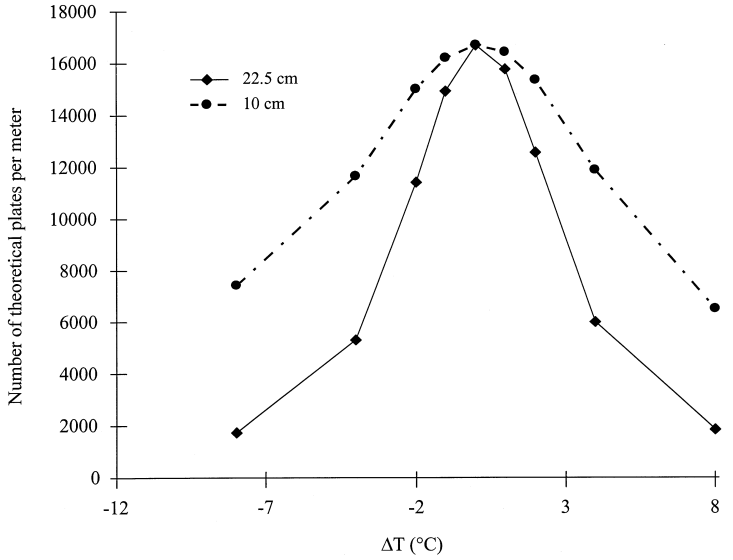

Fig. 14. Calculation of the effect of the bed length on the column efficiency as a function of ΔT. Calculation conditions as indicated in Table 2, except for the column dimensions, changed to 50 mm I.D., variable length and flow-rate (75 ml/min) to match experimental conditions.

close to the wall to go faster than when the column is long where it has the time to compensate the delay. Therefore, the velocity of the sample must be increased when the column is short, and to attain this the temperature of the wall must be warmer than for a long column to allow that difference in velocity.

4.4. Diameter effect

Fig. 15 corresponds to chromatograms calculated for several I.D. columns with the same linear velocity. The temperature of the column wall is 14°C warmer than the temperature of the solvent at the inlet of the column. The internal average temperature profiles are shown in Fig. 4. One can note that the peak corresponding to the analytical column (4.6 mm I.D.) is quite symmetrical despite the value of ΔT. The retention time of that peak indicates that it is eluted at a temperature close to that of the column wall temperature. The chromatograms corresponding to larger-diameter columns present a varying degree of deformation. The percentage of the peak represented by the shoulder decreases when the column diameter increases. This reflects the greater proportion of the solvent which passes through the column uninfluenced by the wall temperature for the larger columns, and indicates that the control of temperature is far more critical for columns of moderate diameter than for large-scale production columns.

5. Conclusion

The calculation of the internal temperature profile in a column shows that for a small-I.D. column (analytical), even if the solvent is at a temperature different from that of the column oven, the separation will be controlled by the temperature of the column wall. For a larger-diameter column, as used for preparative chromatography, a difference in temperature between the wall and the mobile phase, ΔT, can be a real problem. Because the heat transfer in the packed bed is quite slow, a radial temperature gradient will exist in the column and this reduces the column efficiency. The experimental data and the mathematical model presented in this paper show that precautions must be taken when a large-diameter column is used. The effect of ΔT on a column performance is closely related to the flow-rate, the length and the diameter of the column. It is thus necessary to control both the temperature of the mobile phase and of the column wall to ensure good reproducibility and good column performance.

A positive ΔT of a few degrees may be used to

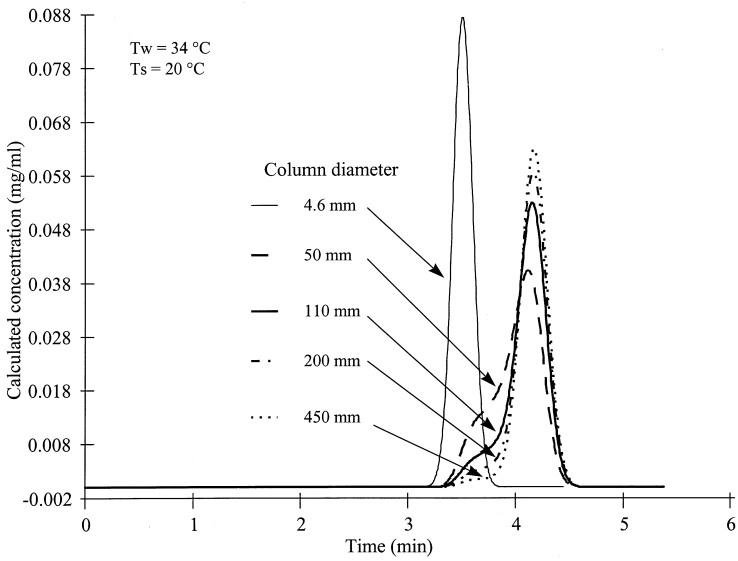

Fig. 15. Calculated chromatograms for different column I.D. with a constant linear velocity of the solvent (0.035 cm/s). Same conditions as Fig. 4; retention and physical properties of the solute and the solvent as indicated in Table 2.

compensate a deformation of the elution band due to the inlet configuration of the column, and thus obtain an optimal efficiency of the column. But this value of ΔT required is a function of the column parameters, the flow-rate and the retention properties of each solute of interest. It is therefore of critical importance that the performance of a column should be measured over a range of ΔT values in order to find the optimum. Equally, the column should be operated at the optimum value of ΔT.

In a future paper the effect of ΔT on preparative separations under non-linear conditions will be presented. A mathematical model will be presented to calculate the chromatogram of a binary separation under non-isothermal conditions and the predictions will be compared with experimental results.

Nomenclature

Greek

α_i	solution of the equation $J_0(x)=0$
δ	reduced temperature in the column
Δ	maximum increase of temperature in the column axis at infinite length
ΔP	pressure drop in the column
ΔT	column wall temperature minus solvent inlet temperature
ϵ_{tot}	total porosity of the column
λ_f	thermal conductivity of the mobile phase
$\overline{\lambda_{lon}}$	axial average thermal conductivity
λ_{rad}	radial average thermal conductivity
λ_s	thermal conductivity of the stationary phase
ρ_m	mobile phase density
$\overline{\rho}$	average density of the heterogeneous system
$\sigma^2_{tot,t}$	variance of the chromatographic peak expressed in time
$\sigma^2_{tot,t,j}$	variance of the chromatographic peak in the elementary column j expressed in time
ν	reduced velocity in the column $=u_0 d_p/D_m$
ξ	reduced length
ξ_L	reduced length for $z=L_{col}$

Roman

A, B, C	parameters of the Knox equation
C_j	concentration of solute in the mobile phase in an elementary column j
C_{inj}	concentration in the injection
$\overline{C_p}$	average specific heat of the heterogeneous system
C_{pm}	specific heat of the mobile phase
d_p	average particle size
D_m	diffusion coefficient of the solute
$f(t)$	function to fit the chromatographic peak
h	reduced plate height
j	index of an elementary column
$J_0(x)$	Bessel function of the zero order
$J_1(x)$	Bessel function of the first order
$k'j$	retention factor of solute in an elementary column j
l_{relax}	relaxation length
L_{col}	column length
N_{col}	number of theoretical plates or column efficiency
p	pressure in the porous bed
Q_v	volumetric flow-rate
r	radial position
$r_{0.1}$	radial position for $\delta=0.1$
r^2	correlation coefficient for linear regression
R_c	column radius
S_j	cross section of an elementary column
t	time
$t_{0,j}$	retention time of an unretained compound in an elementary column j
t_{th}	time required for the heat to diffuse from the wall
t_R	retention time of a retained compound
$t_{R,j}$	retention time of a retained compound in an elementary column j
T	temperature (K)
T_s	solvent temperature at the column inlet
T_w	column wall temperature
ν_s	linear velocity of the solvent
$W_{1/2}$	width of the peak measured at half of the height
z	axial co-ordinate

References

[1] J.J. van Deemter, V.J. Zuiderweg, A. Klinkenberg, Chem. Eng. Sci. 5 (1956) 271–289.
[2] J.H. Knox, G.R. Laird, P.A. Raven, J. Chromatogr. 122 (1976) 129–145.
[3] J.H. Knox, J. Chromatogr. Sci. 15 (1977) 352–364.
[4] M. Martin, C. Eon, G. Guiochon, J. Chromatogr. 108 (1975) 229–241.
[5] J.J. Kirkland, W.W. Yau, H.J. Stoklosa, C.H. Dilks Jr., J. Chromatogr. Sci. 15(8) (1977) 303–316.
[6] L.R. Snyder, J.J. Kirkland, in: Modern Preparative Liquid Chromatography, 2nd ed., Wiley-Interscience, New York, 1979.
[7] M.J.E. Golay, J.G. Atwood, J. Chromatogr. 186 (1979) 353–370.
[8] M. Martin, G. Guiochon, C.R. Acad. Sci. Paris 294 (1982) 899–902.
[9] S.G. Weber, P.W. Carr, in: P.R. Brown, R.A. Hartwick (Eds.), High Performance Liquid Chromatography, Ch. 1, Wiley-Interscience, New York, 1988.
[10] R.C. Simpson, in: P.R. Brown, R.A. Hartwick (Eds.), High Performance Liquid Chromatography, Ch. 9, Wiley-Interscience NY, 1988.
[11] H. Colin, in: P.R. Brown, R.A. Hartwick (Eds), High Performance Liquid Chromatography, Ch. 11, Wiley-Interscience NY, 1988.
[12] H. Colin, in: Eli Grushka (Ed.), Preparative Scale Chromatography, Ch. 3, Marcel Dekker, NY, 1989.
[13] B. Coq, G. Cretier, J.L. Rocca, R. Kastener, J. Chromatogr. 178 (1979) 41–61.
[14] E. Singer, R.H. Wilhelm, Chem. Eng. Prog. 46 (1950) 343–357.
[15] S. Abbott, P. Achener, R. Simpson, F. Klink, J. Chromatogr. 218 (1981) 123–135.
[16] H.J. Lin, S. Horvath, Chem. Eng. Sci. 36 (1981) 47–55.
[17] H. Poppe, J.C. Kraak, J.F.K. Huber, J.H.M. van den Berg, Chromatographia 14(9) (1981) 515–523.
[18] H. Poppe, J.C. Kraak, J. Chromatogr. 282 (1983) 399–412.
[19] O. Dapremont, G.B. Cox, H. Colin, P. Hilaireau, M. Martin, Presented at PREP'94, Baden-Baden, 1994.
[20] A. Brandt, G. Mann, W. Arlt, submitted for publication in J. Chromatogr. A.
[21] O. Dapremont, G.B. Cox, H. Colin, P. Hilaireau, M. Martin, Presented at PREP'96, Basel, 1996.
[22] T. Welsch, M. Schmid, J. Kutter, A. Kálmán, J. Chromatogr. A 728 (1996) 299–306.
[23] T. Yun, G. Guiochon, J. Chromatogr. A 734 (1996) 97–103.
[24] B. Ooms, LC·GC 14(4) (1996) 306–324.
[25] R.H. Perry, D.W. Green, in: Perry's Chemical Engineers' Handbook, 6th ed., McGraw-Hill, New York, 1984.